Quantification of Active Sites for the Determination of Methanol Oxidation Turn-over Frequencies Using Methanol Chemisorption and in Situ Infrared Techniques. 1. Supported Metal Oxide Catalysts

Loyd J. Burcham,[†] Laura E. Briand,[‡] and Israel E. Wachs*,[§]

Zettlemoyer Center for Surface Studies and Department of Chemical Engineering, Lehigh University, Bethlehem, Pennsylvania 18015, and Centro de Investigacion y Desarrollo en Procesos Cataliticos, Universidad Nacional de La Plata, Calle 47 No. 257, (1900) La Plata, Argentina

Received January 4, 2001. In Final Form: May 8, 2001

Methanol oxidation over metal oxide catalysts is industrially important for the production of formaldehyde, but knowledge about the intrinsic catalysis taking place is often obscured by a lack of knowledge as to the number of active sites present on the catalyst surface. In the present study, the number of surface sites active in methanol oxidation has been determined over a wide range of supported metal oxide catalysts using quantitative methanol chemisorption and in-situ infrared titration techniques performed at an experimentally optimized temperature of 110 °C. It was found that a steric limitation of about 0.3 methoxylated surface species (e.g., strongly Lewis-bound CH_3OH_{ads} and dissociatively adsorbed $-OCH_{3,ads}$, which are the reactive surface intermediates in methanol oxidation) exists per active deposited metal oxide metal atom across all supported metal oxides. Hence, the use of methanol chemisorption for counting active surface sites is more realistic than other site-counting methods for the kinetic modeling of methanol oxidation, where during steady-state reaction the departure of the actual coverage of methoxylated surface intermediates from the maximum saturation surface coverage is of critical importance. Methanol oxidation turn-over frequencies (TOF = methanol molecules converted per second per active surface site) calculated using these new methanol chemisorption surface site densities increased by a factor of ∼3 the TOFs estimated in previous studies using the total number of deposited metal oxide metal atoms. Nevertheless, the support effect observed previously (TOFs for MoO_3 and V_2O_5 supported on oxides of Zr ∼ Ce > Ti > Al ≫ Si) remains virtually unchanged as a general trend in the present study and correlates with the support cation electronegativity via bridging M−O−Support bonds. The methanol chemisorption technique may now be used with confidence to search for similar ligand effects in bulk metal oxides, where counting active sites has traditionally been very difficult (subject of part 2, Burcham, L. J.; Briand, L. E.; Wachs, I. E. *Langmuir* **2001**, *17*, 6175, of the present two-paper series).

Introduction

The ability to quantitatively determine and control the number of active metal oxide surface sites in supported and bulk metal oxide catalysts remains a great challenge to the formulation of fundamental structure−reactivity relationships in these systems. When available, knowledge of the active site density allows for direct comparison of intrinsic catalytic activities across different catalysts, as expressed by their turn-over frequencies (TOF = molecules converted per second per *active surface metal oxide site*).[1] Active site density and TOF measurements are routinely performed on bulk metal and supported metal catalysts using chemisorption of probe molecules such as CO, H_2, and O_2 to quantify the active metal surface area.[2] Unfortunately, the chemisorption of these probe molecules is very difficult on metal oxide surfaces. The use of probe molecules that are more easily chemisorbed onto oxides can provide alternative methods for quantifying site densities in metal oxide catalysts. Methanol is a particularly good choice due to the commercial importance of the methanol oxidation reaction to formaldehyde over bulk $Fe_2(MoO_4)_3-MoO_3$ mixtures,[3] and for its fundamental scientific importance as a probe of metal oxide catalytic properties in general.[4]

Supported metal oxide catalysts, which consist of an active metal oxide (MoO_3, V_2O_5, Cr_2O_3, Nb_2O_5, Re_2O_7, WO_3, etc.) molecularly dispersed as a two-dimensional surface metal oxide overlayer on a high surface area oxide support (Al_2O_3, SiO_2, TiO_2, ZrO_2, CeO_2, MgO, etc.), may serve as model reference systems for the development of a quantitative methanol chemisorption technique because their active surface metal oxide site densities and methanol oxidation TOF's have been successfully determined using other methods.[5,6] In these catalytic systems, the problems associated with measuring surface site densities by selective chemisorption of probe molecules are circumvented because the number of active surface sites may be taken directly as the number of metal atoms deposited on the oxide support surface. At monolayer coverage, monolayer being defined as the maximum metal oxide loading

* Corresponding author. Phone: 610-758-4274. Fax: 610-758-6555. E-mail: iew0@lehigh.edu.

[†] Present address: Congoleum Corporation,P.O. Box 3127 , Mercerville, NJ 08619.

[‡] Centro de Investigacion y Desarrollo en Procesos Cataliticos.

[§] Zettlemoyer Center for Surface Studies and Department of Chemical Engineering.

(1) Thomas, J. M.; Thomas, W. J. *Principles and Practice of Heterogeneous Catalysis*; VCH Publishers: New York, 1997.

(2) Ribeiro, F. H.; Schach von Wittenau, A. E.; Bartholomew, C. H.; Somorjai, G. A. *Catal. Rev.−Sci. Eng.* **1997**, *39*, 49.

(3) Gerberich, H. R.; Seaman, G. C. Formaldehyde. In *Kirk-Othmer Encyclopedia of Chemical Technology*, 4th ed.; John Wiley and Sons: New York, 1994; Vol. 11, pp 929−951.

(4) Tatibouët, J. M. *Appl. Catal. A* **1997**, *148*, 213.

(5) Wachs, I. E.; Deo, G.; Vuurman, M. A.; Hu, H.; Kim, D. S.; Jehng, J. M. *J. Mol. Catal.* **1993**, *82*, 443.

(6) Wachs, I. E. *Catal. Today* **1996**, *27*, 437.

10.1021/la010009u CCC: $20.00
Published on Web 09/08/2001

that produces only two-dimensional surface species and not bulk metal oxide microcrystallites (as measured by Raman spectroscopy), the surface site densities typically correspond to 4−5 metal atoms/nm^2 (6.6−8.3 μmol metal atoms/m^2) for MoO_3, WO_3, Nb_2O_5, and CrO_3 on all supports.[6] Vanadia surface species appear to pack more efficiently on the oxide support surface, forming about 8 V atoms/nm^2 (13 μmol metal atoms/m^2), while the volatility of rhenia dimers limits its coverage to about half of a predicted monolayer (~2 Re atoms/nm^2, or 3.3 μmol metal atoms/m^2). The inertness of the silica surface prevents monolayer coverages of deposited metal oxides from being achieved on this oxide support (about 0.5 deposited metal atoms/nm^2, or 0.8 μmol metal atoms/m^2, being typical before forming bulk oxide microcrystallites of the deposited metal oxide). However, recent synthesis methods have allowed the creation of very highly dispersed surface vanadia on silica (2.6 V atom/nm^2, or 4.3 μmol metal atoms/m^2).[7]

Indeed, such information about active surface site densities in supported metal oxides and the difficulty in obtaining this information for bulk metal oxides[8] has meant that much of the current fundamental structure−reactivity knowledge concerning methanol oxidation on metal oxides has been derived from studies of supported metal oxide systems. In particular, the works by Wachs et al.[9,10] and Niwa et al.[11−13] for MoO_3 dispersed over many different supports have revealed a fundamental support effect upon the TOF to partial oxidation products in methanol oxidation. They observed an order of magnitude difference in TOF over monolayer molybdena catalysts, the more electropositive supports providing the greater specific activity: $ZrO_2 \sim TiO_2 \gg Nb_2O_5 > Al_2O_3 > SiO_2$[9], $ZrO_2 > TiO_2 > Al_2O_3$[13], and $SnO_2 > Fe_2O_3 \sim ZrO_2 > TiO_2 > Al_2O_3$.[11] The support effect in supported vanadia catalysts is even greater than that in the corresponding Mo-based catalysts, spanning 3 orders of magnitude.[14−26] As with supported molybdena, the more electropositive support cations yield the greatest TOFs to formaldehyde. Under 6% methanol, the TOFs for catalysts at monolayer coverages were found to be highest for vanadia on ceria ($1.0 \times 10^{+0}$ s^{-1}), followed by V_2O_5/ZrO_2 (1.7×10^{-1} s^{-1}) and V_2O_5/TiO_2 (1.1×10^{-1} s^{-1}), and were much lower for V_2O_5/Al_2O_3 (6.8×10^{-3} s^{-1}).[20] Explanations for this support effect have included correlations of the TOF with the support cation electronegativity,[21] H_2 TPR peak temperatures,[9,14,22] and UV−vis DRS ligand−metal charge-transfer edge energies (the latter technique having been applied to the related reaction of oxidative propane dehydrogenation, which has certain mechanistic differences compared to methanol oxidation).[17]

These relationships, based upon quantification of the total number of active metal oxide surface sites, have provided a great deal of insight into the nature of methanol oxidation over supported metal oxide catalysts. However, steric and lateral interaction hindrances can potentially reduce the actual maximum number of *simultaneously* reacting active metal oxide surface sites to a fraction of the total number of active metal oxide surface sites. In the case of methanol oxidation over metal oxides, the maximum number of *simultaneously* reacting active metal oxide surface sites is limited to the saturation number of methoxylated surface species, e.g., $OCH_{3,ads}$ and CH_3OH_{ads}, which are the reactive surface intermediates in methanol oxidation.[27−30] Methanol chemisorption on metal oxide catalysts, in which methanol is quantitatively adsorbed onto the metal oxide surface to form these methoxylated surface species, can provide a feasible method for active site determinations. Indeed, the gravimetrically quantified methanol chemisorption works of Farneth et al.[31−33] and Sleight et al.[34] over bulk metal oxides are discussed in detail in part 2[8] of the present two-paper study.[8] However, the active site determinations presented in these gravimetric investigations have been complicated by questions relative to the stoichiometry of methanol adsorption and by questions regarding the choice of adsorption temperature.[8] These complications emphasize the need for further work and additional experimental techniques for determining active surface site densities with methanol chemisorption over metal oxides.

Finally, a number of related studies have quantitatively measured the adsorption isotherms of methanol on metal oxides using IR, calorimetric, gravimetric, and volumetric methods, although not necessarily for the purpose of active site determinations. Generally, the isotherms were of either the Langmuir type (Al_2O_3,[35] Cr_2O_3,[36] MgO,[37] β-MoO_3,[31] SiO_2,[38] TiO_2,[39] and ZnO[40]), the Elovich/Temkin

(7) Gao, X.; Bare, S. R.; Weckhuysen, B. M.; Wachs, I. E. *J. Phys. Chem. B* **1998**, *102*, 10842.
(8) Burcham, L. J.; Briand, L. E.; Wachs, I. E. *Langmuir* **2001**, *17*, 6175.
(9) Hu, H.; Wachs, I. E. *J. Phys. Chem.* **1995**, *99*, 10911.
(10) Kim, D. S.; Wachs, I. E.; Segawa, K. *J. Catal.* **1994**, *146*, 268.
(11) Niwa, M.; Sano, M.; Yamada, H.; Murakami, Y. *J. Catal.* **1995**, *151*, 285.
(12) Yamada, H.; Niwa, M.; Murakami, Y. *Appl. Catal. A* **1993**, *96*, 113.
(13) Matsuoka, Y.; Niwa, M.; Murakami, Y. *J. Phys. Chem.* **1990**, *94*, 1477.
(14) Arena, F.; Frusteri, F.; Parmaliana, A. *Appl. Catal. A* **1999**, *176*, 189.
(15) Deo, G.; Wachs, I. E.; Haber, J. *Crit. Rev. Surf. Chem.* **1994**, *4*, 141.
(16) Burcham, L. J.; Wachs, I. E. *Catal. Today* **1999**, *49*, 467.
(17) Khodakov, A.; Olthof, B.; Bell, A. T.; Iglesia, E. *J. Catal.* **1999**, *181*, 205.
(18) Inumaru, K.; Misono, M.; Okuhara, T. *Appl. Catal. A* **1997**, *149*, 133.
(19) Wachs, I. E.; Weckhuysen, B. M. *Appl. Catal. A* **1997**, *157*, 67.
(20) Wachs, I. E.; Deo, G.; Juskelis, M. V.; Weckhuysen, B. M. In *Dynamics of Surfaces and Reaction Kinetics in Heterogeneous Catalysis*; Froment, G. F., Waugh, K. C., Eds.; Elsevier: Amsterdam, 1997; pp 305−314.
(21) Wachs, I. E. In *Catalysis*; Spivey, J. J., Ed.; The Royal Society of Chemistry: Cambridge, 1997; Vol. 13, pp 37−54.
(22) Deo, G.; Wachs, I. E. *J. Catal.* **1994**, *146*, 323.
(23) Deo, G.; Wachs, I. E. *ACS Symp. Ser.* **1993**, *523*, 31.
(24) Deo, G.; Wachs, I. E. *J. Catal.* **1991**, *129*, 307.
(25) Kijenski, J.; Baiker, A.; Glinski, M.; Dollenmeier, P.; Wokaun, A. *J. Catal.* **1986**, *101*, 1.
(26) Roozeboom, F.; Cordingley, P. D.; Gellings, P. J. *J. Catal.* **1981**, *68*, 464.
(27) Lavalley, J. C. *Catal. Today* **1996**, *27*, 377.
(28) Busca, G. *Catal. Today* **1996**, *27*, 457.
(29) Busca, G.; Elmi, A. S.; Forzatti, P. *J. Phys. Chem.* **1987**, *91*, 5263.
(30) Holstein, W. L.; Machiels, C. J. *J. Catal.* **1996**, *162*, 118.
(31) Farneth, W. E.; McCarron, E. M.; Sleight, A. W.; Staley, R. H. *Langmuir* **1987**, *3*, 217.
(32) Farneth, W. E.; Staley, R. H.; Sleight, A. W. *J. Am. Chem. Soc.* **1986**, *108*, 2327.
(33) Farneth, W. E.; Ohuchi, F.; Staley, R. H.; Chowdhry, U.; Sleight, A. W. *J. Phys. Chem.* **1985**, *89*, 2493.
(34) Cheng, W.-H.; Chowdhry, U.; Ferretti, A.; Firment, L. E.; Groff, R. P.; Machiels, C. J.; McCarron, E. M.; Ohuchi, F.; Staley, R. H.; Sleight, A. W. In *Heterogeneous Catalysis (Proceedings of the Second Symposium of the IUCCP of the Department of Chemistry, Texas A&M)*; Shapiro, B. L., Ed.; Texas A&M University Press: College Station, TX, 1984; p 165.
(35) Busca, G.; Rossi, P. F.; Lorenzelli, V.; Benaissa, M.; Travert, J.; Lavalley, J.-C. *J. Phys. Chem.* **1985**, *89*, 5433.
(36) Kittaka, S.; Umezu, T.; Ogawa, H.; Maegawa, H.; Takenaka, T. *Langmuir* **1998**, *14*, 832.
(37) Spitz, R. N.; Barton, J. E.; Barteau, M. A.; Staley, R. H.; Sleight, A. W. *J. Phys. Chem.* **1986**, *90*, 4067.
(38) (a) Borello, E.; Zecchina, A.; Morterra, C. *J. Phys. Chem.* **1967**, *71*, 2938. (b) Borello, E.; Zecchina, A.; Morterra, C.; Ghiotti, G. *J. Phys. Chem.* **1967**, *71*, 2945.
(39) Rossi, P. F.; Busca, G. *Colloids Surf.* **1985**, *16*, 95.

type (α-MoO_3[31−33] and ZnO[37]), or BET type II (MgO[41] and TiO_2[42]). Other isotherm and saturation coverages are found elsewhere for CeO_2,[43] MoO_3,[44,45] heteropoly-Mo,[46] TiO_2,[47,48] and ZrO_2.[49] Generally, the Langmuir isotherm applies to chemisorption on uniform surfaces, the Elovich/Temkin isotherm best fits surfaces with very heterogeneous surface sites and heterogeneous adsorption energies, and the BET type II isotherm applies to multilayer adsorption encountered in physical adsorption.[50] Also, methoxy infrared extinction coefficients have been reported for CeO_2,[43] MoO_3,[44] ZnO, MgO,[37] SiO_2,[38] and ZrO_2,[51] although the values vary considerably due to the different choices of frequency and bandwidth chosen for integration by the various authors. The different experimental conditions employed in these studies (temperature, pressure, etc.) also severely limit side-by-side comparisons of results from different studies.

In the present study (part I of a two-paper series), the objectives are to develop a general method for counting the number of active surface metal oxide sites and for calculating methanol oxidation TOF's in supported metal oxide catalysts using quantitative methanol chemisorption and infrared spectroscopy. Infrared spectroscopy has been chosen as the detection method, in part, because the adsorbed surface methoxy species produce strong IR signals. More importantly, and unlike other "blind" gravimetric, calorimetric, or volumetric methods that require assumptions about adsorption stoichiometry or require separate experimental measurements to account for water produced upon adsorption,[8,31−34] the use of IR spectroscopy can quantify the surface methoxy species directly. Methanol has been chosen as the probe molecule because of its high reactivity toward oxides (unlike CO, H_2, and O_2) and its relevance to the methanol oxidation reaction.

2. Experimental Section

2.1. Catalyst Preparation. The supported metal oxide catalysts used in this study were prepared by the incipient wetness impregnation method. This technique is described in detail elsewhere,[5,7,10,22,52−55] so only a brief summary is given here. The supports (γ-Al_2O_3 with 250 m^2/g from Engelhard or 180 m^2/g from Harshaw, P-25 TiO_2 with 55 m^2/g from Degussa, CeO_2 with 36 m^2/g from Engelhard, SiO_2 with 320 m^2/g from Cabot, and ZrO_2 with 39 m^2/g from Degussa) were first calcined to 723−773 K and then cooled to room temperature. The supports were then impregnated with aqueous solutions of ammonium heptamolybdate, ammonium metatungstate, chromium nitrate, 60−70 wt % perrhenic acid, or niobium oxalate. The moisture sensitive vanadia precursor, vanadium triisopropoxide, was mixed with methanol to achieve incipient wetness under a nitrogen atmosphere inside a glovebox. After thorough mixing, the samples were dried at room temperature in air (in a glovebox for vanadia samples) for 16 h, followed by heating to 393 K (under flowing nitrogen for vanadia samples) for 12 h. Finally, the samples were calcined to 723 K (TiO_2, CeO_2, SiO_2, and ZrO_2 samples) and 773 K (Al_2O_3 samples) in pure oxygen for 4 h.

All supported catalysts correspond to approximately monolayer coverages, except that the relatively inert silica surface and the volatilization of rhenia dimers prevents attainment of complete monolayers in these systems. Instead, these systems contain the highest loading possible of deposited oxide that does not form bulk metal oxide microcrystallites (silica supported systems) or volatilize as dimers (rhenia catalysts). On all supported metal oxide samples, the presence of monolayer dispersion (or submonolayer dispersion in the case of silica-supported and rhenia systems) and the absence of deposited metal oxide microcrystallites were verified with Raman spectroscopy (see ref 56 for experimental details). Surface areas were determined with BET instrumentation (Quantachrome Corp., Quantasorb model OS-9).

2.2. In Situ Infrared Experiments. The in situ infrared experiments were performed with a BioRad FTS-40A FTIR spectrometer equipped with a DTGS detector. The infrared spectra were recorded at a resolution of 2 cm^{-1} using 250 signal-averaged scans and, when necessary, were smoothed using the Savitsky−Golay method. The IR was operated in transmission mode using a specially designed in situ cell that has been previously described.[16] Transmission mode was selected for this work due to the linear absorbance signal dictated by Beer's law, and due to the inherent difficulties involved in quantitative reflectance methods such as DRIFTS (diffuse reflectance) and ATR (attenuated total reflectance). Calibration of the surface methoxy IR signal was achieved by quantitatively dosing known amounts of methanol onto the catalysts at 110 °C under vacuum. For this purpose, a dosing volume of 3.19 mL was attached directly above the IR cell and connected to a vacuum manifold (Alcatel mechanical pump and Varian HS-2 diffusion pump; MKS Pirani and Cold Cathode pressure gauges; ultimate vacuum ∼10^{-6} Torr). Pressure in the dosing volume (T = 25 °C) was measured with a high accuracy capacitance manometer (MKS Baratron) and varied between 0.5 and 20 Torr of methanol. Methanol (Alfa Aesar, semiconductor grade) was supplied from a source at room temperature that was purged of headspace gases by freezing of the methanol with liquid nitrogen followed by evacuation.

The following experimental procedure was employed. Samples of ∼30−60 mg were first pressed (∼40 000 psi) into self-supporting catalyst wafers that were thin enough that significant IR transmission was possible. Some samples that were nearly impossible to press into self-supporting wafers were instead pressed into thin disks of perforated stainless steel (30% open area and ∼5−30 mg of catalyst). After being weighed and loaded into the IR cell, the samples were heated in situ to 350 °C in flowing oxygen (16 mL/min; ultrahigh purity; JWS Technologies) and helium (84 mL/min; ultrahigh purity; JWS Technologies). The pretreated catalysts were then cooled to 110 °C, and the IR cell was evacuated to ∼10^{-5} Torr. After the collection of a clean spectrum, methanol was quantitatively adsorbed onto the catalyst in steps (∼1 μmole methanol in each step) with IR spectra recorded after each stepwise addition.

Saturation of the surface with methoxylated surface species was indicated by a leveling off of the signal vs concentration curve due to the formation of physisorbed and gas-phase methanol species (gas-phase IR band at 1033 cm^{-1}). The stepwise quantitative adsorption was carried out at 110 °C to ensure that the methanol only adsorbed as strongly bound methoxylated surface species (otherwise, the known μmoles of methanol introduced onto the sample would not correspond to the micromoles of

(40) (a) Nagao, M.; Morimoto, T. *J. Phys. Chem.* **1980**, *84*, 2054. (b) Morimoto, T.; Kiriki, M.; Nagao, M. *J. Phys. Chem.* **1980**, *84*, 2058.
(41) Liang, S. H. C.; Gay, I. D. *Langmuir* **1985**, *1*, 593.
(42) Suda, Y.; Morimoto, T.; Nagao, M. *Langmuir* **1987**, *3*, 99.
(43) (a) Badri, A.; Binet, C.; Lavalley, J.-C. *J. Chem. Soc., Faraday Trans.* **1997**, *93*, 1159. (b) Binet, C.; Daturi, M.; Lavalley, J.-C. *Catal. Today* **1999**, *50*, 207.
(44) Groff, R. P. *J. Catal.* **1984**, *86*, 215.
(45) Ohuchi, F.; Firment, L. E.; Chowdhry, U.; Ferretti, A. *J. Vac. Sci. Technol. A* **1984**, *2*, 1022.
(46) Farneth, W. E.; Staley, R. H.; Domaille, P. J.; Farlee, R. D. *J. Am. Chem. Soc.* **1987**, *109*, 4018.
(47) Lusvardi, V. S.; Barteau, M. A.; Farneth, W. E. *J. Catal.* **1995**, *153*, 41.
(48) Kim, K. S.; Barteau, M. A.; Farneth, W. E. *Langmuir* **1988**, *4*, 533.
(49) Bianchi, D.; Chafik, T.; Khalfallah, M.; Teichner, S. J. *Appl. Catal. A* **1995**, *123*, 89.
(50) (a) Carberry, J. J. *Chemical and Catalytic Reaction Engineering*; McGraw-Hill: New York, 1976; pp 378−382. (b) Zhang, W.; Oyama, S. T.; Holstein, W. L. *Catal. Lett.* **1996**, *39*, 67.
(51) (a) Ouyang, F.; Kondo, J. N.; Maruya, K.; Domen, K. *J. Phys. Chem. B* **1997**, *101*, 4867. (b) Ouyang, F.; Kondo, J. N.; Maruya, K.; Domen, K. *Catal. Lett.* **1998**, *50*, 179.
(52) Kim, D. S.; Wachs, I. E. *J. Catal.* **1993**, *141*, 419.
(53) (a) Ostromecki, M. M.; Burcham, L. J.; Wachs, I. E.; Ramani, N.; Ekerdt, J. *J. Mol. Catal. A* **1998**, *132*, 59. (b) Ostromecki, M. M.; Burcham, L. J.; Wachs, I. E. *J. Mol. Catal. A* **1998**, *132*, 43.
(54) Kim, D. S.; Wachs, I. E. *J. Catal.* **1993**, *142*, 166.
(55) Jehng, J.-M.; Wachs, I. E. *Catal. Today* **1990**, *8*, 37.
(56) Burcham, L. J.; Wachs, I. E. *Spectrochim. Acta Part A* **1998**, *54*, 1355.

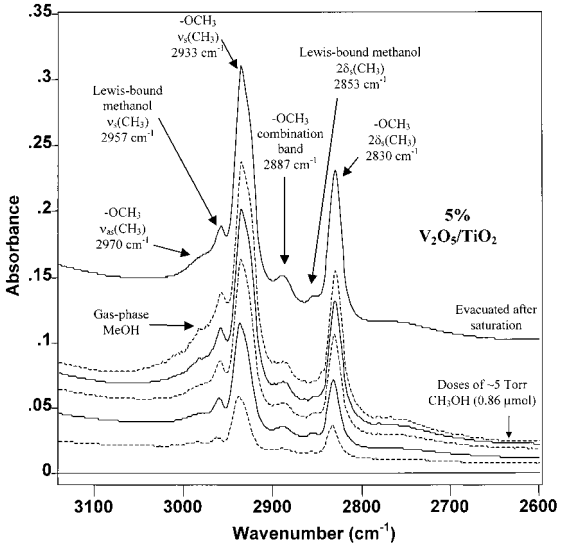

Figure 1. Quantitative methanol dosing experiment on 5% V_2O_5/TiO_2 at 110 °C. Spectra shown are difference spectra from which the clean catalyst spectrum has been subtracted.

catalytically relevant methoxylated surface species). At lower adsorption temperatures, the methanol adsorbs to form both strongly bound methoxylated surface species and weakly bound physisorbed methanol, while at higher temperatures the methoxylated surface species react to form formaldehyde and other products. Finally, the spectrum of the catalyst completely saturated with chemisorbed methoxylated surface species was obtained by exposing the sample to 10 Torr of methanol for 10 min, followed by evacuation and spectrum acquisition.

2.3. Methanol Oxidation Activity. Catalytic data were obtained using an isothermal fixed-bed reactor operated under differential conditions, following a similar procedure as described in ref 22. Powdered samples of 10−60 mg and 75 μm particle size were packed inside glass reactor tubes that were heated by a furnace to 250 °C. A flow of $CH_3OH/O_2/He$ (molar ratio of 6/13/81) was passed over the catalyst at a rate of 100 mL/min, and product analysis was performed with an HP 5890 Series II gas chromatograph equipped with FID and TCD detectors. Columns in the GC included a Carboxene-1000 packed column for TCD detection and a CP-sil 5CB capillary column for the FID detector. Sample pretreatment involved heating the catalyst to 450 °C under O_2/He for 30 min prior to beginning the methanol flow.

3. Results

3.1. IR Spectra and Band Assignments. The experimental results and calculations are presented in Figures 1−8 and in Tables 1−4. The IR spectra of the surfaces prior to CH_3OH adsorption have been subtracted from the spectra of methanol-exposed surfaces in order to isolate the surface signals arising from methanol chemisorption. Infrared spectral results from a typical dosing experiment are given in Figure 1 for the C−H stretching region of methanol-dosed 5% V_2O_5/TiO_2. In this figure, methanol adsorption to methoxylated surface species is indicated by the appearance of four intense, sharp bands at ~2950/2930 and ~2850/2830 cm^{-1}, as well as two weak and broad bands at ~2890 and ~2970 cm^{-1}. In addition, three bands appear in the lower frequency region at 1447, 1435, and ~1065 cm^{-1} (see Figure 2; methanol-dosed 5% V_2O_5/TiO_2 spectrum). Assignments for these vibrational modes must begin by recognizing that there are two distinctly different methoxylated surface species present: an intact, methanol-like species (species I) and a dissociated surface methoxy species (species II, $-OCH_3$). While many authors have previously assigned Species I to weakly bound physisorbed methanol,[37,44,57,58] the temperature and evacuation stability of this species indicates

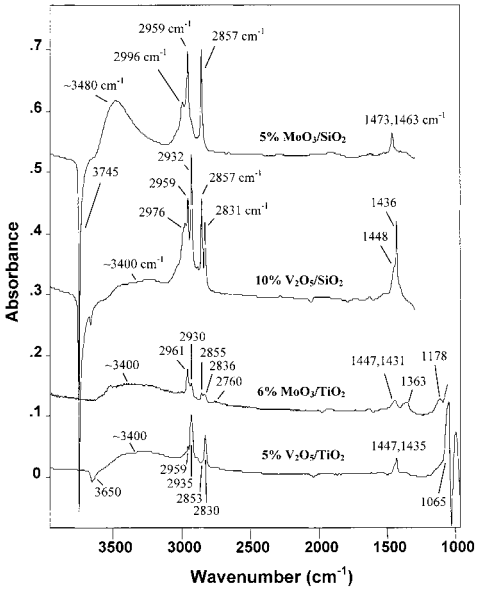

Figure 2. Difference spectra (normalized to 10 mg) of adsorbed methoxylated surface species present on silica-supported MoO_3 and V_2O_5, as well as on titania-supported MoO_3 and V_2O_5. Note the differences in the ratios of species I vs species II.

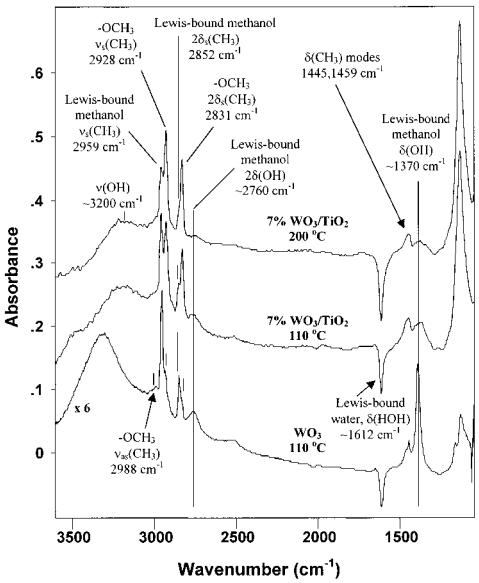

Figure 3. Difference spectra (normalized to 10 mg) of adsorbed methoxylated surface species on tungsten oxide catalysts, which produce large amounts of Lewis-bound methanol (species I).

that it must instead be due to a much stronger Lewis-coordinated methanol adduct on surface metal cations (Lewis acid sites).[35,38,59,60] The same conclusion has also been reached by Lavalley[27] and Busca[28] in recent reviews of the adsorption of alcohols and other probe molecules on metal oxides.

In the present study, the existence of such Lewis-bound surface methanol species is best illustrated by the tungsten oxide systems, which are well-known to have a high surface density of Lewis acid sites.[61] Figure 3 shows that these

(57) Beebe, T. P.; Crowell, J. E.; Yates, J. T. *J. Phys. Chem.* **1988**, *92*, 1296.
(58) Groff, R. P.; Manogue, W. H. *J. Catal.* **1984**, *87*, 461.
(59) Ramis, G.; Busca, G.; Lorenzelli, V. *J. Chem. Soc., Faraday Trans.* **1987**, *83*, 1591.
(60) Busca, G.; Lorenzelli, V. *J. Catal.* **1980**, *66*, 155.
(61) Berholc, J.; Horsley, J. A.; Murrell, L. L.; Sherman, L. G.; Soled, S. *J. Phys. Chem.* **1987**, *91*, 1526.

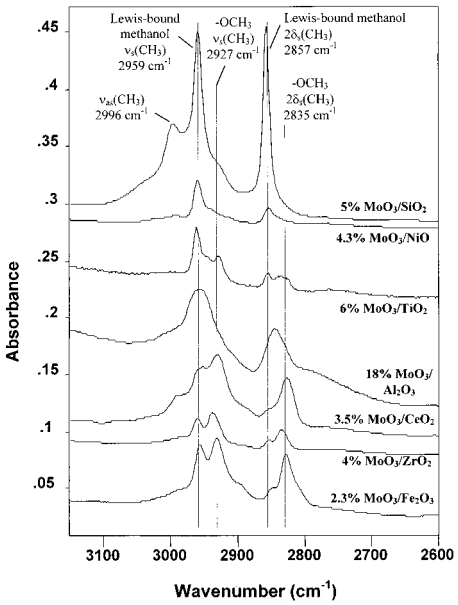

Figure 4. Difference spectra (normalized to 10 mg) of adsorbed methoxylated surface species on supported molybdena catalysts in the C−H stretching region.

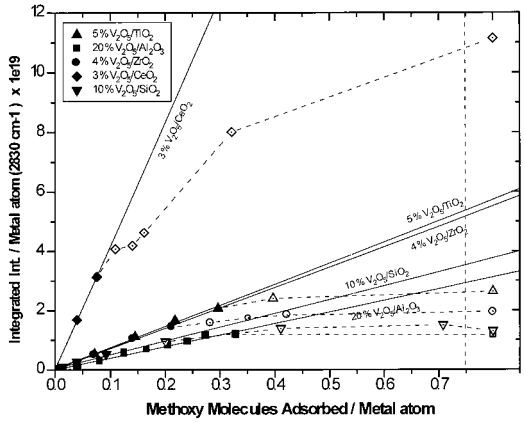

Figure 5. Illustration of the data reduction procedure performed on supported vanadia catalysts. Integrated molar extinction coefficients are determined from the linear portion of the plot of integrated absorbance (2830−2850 cm^{-1} region) vs amount of methanol adsorbed to methoxylated surface species.

systems possess a number of vibrational bands associated with the OH group of intact species I: a strong band at ∼1370 cm^{-1} due to the OH bending mode, δ(O−H); the overtone, 2δ(O−H), of this OH bending mode at ∼2760 cm^{-1}; and O−H stretching modes, ν(O−H), in the region 3100−3500 cm^{-1}.[27,28,35,38,59,60] The main C−H stretching modes of this methanol species occur at 2950 and 2850 cm^{-1} (see assignments below). This intact, Lewis-bound surface methanol species is present at 110 °C under ∼10^{-5} Torr of vacuum in both bulk WO_3 and in 7% WO_3/TiO_2 and persists in the latter catalyst to 200 °C, although with a noticeable reduction in band intensities. A band at 1612 cm^{-1} is due to the δ(H−O−H) mode of strongly Lewis-bound water,[62−64] which is present on these catalysts even after evacuation at temperatures as high as 200 °C. Its disappearance after methanol adsorption is indicated in Figure 3 by a negative peak and demonstrates that the

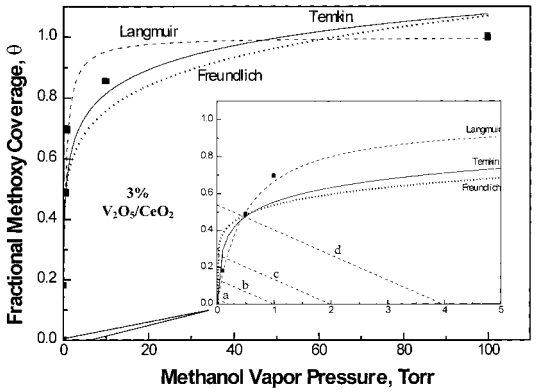

Figure 6. Equilibrium isotherm data for methanol chemisorption on 3% V_2O_5/CeO_2. The insert shows the low-pressure region with mass-balances intersecting the isotherm at different equilibrium coverages for different initial pressures in the dosing chamber (a = 1 Torr, b = 5 Torr, c = 10 Torr, and d = 20 Torr). Note that the x-axis represents the pressure of the IR cell and dosing chamber combined volume, so the P_o initial pressures indicated along the x-axis ($\theta = 0$) at the mass balance x-intercepts are considerably *lower* than their corresponding initial pressures, a−d, in the dosing chamber before exposure to the IR cell.

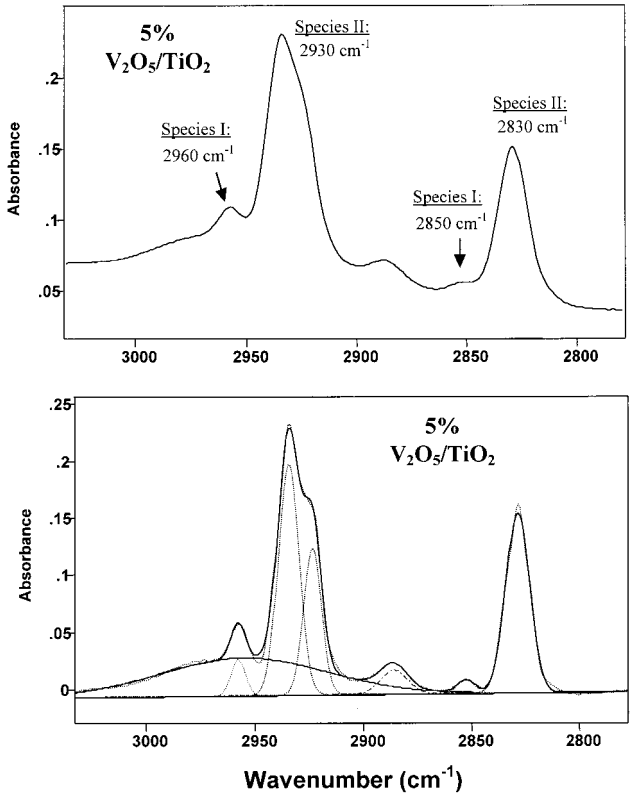

Figure 7. Fourier Self-Deconvolution of C−H stretching bands in 5% V_2O_5/TiO_2. The upper plot shows the raw difference spectrum and the lower plot shows the results of deconvolution and curve fitting with Voigt profiles.

adsorption of methanol displaces Lewis-bound water. The absence of such a negative band in the spectra of Figure 2 is representative of the fact that much less Lewis-bound water was present under the same experimental conditions for the other tested catalysts. In addition, the higher affinity of the oxide surfaces for methanol relative to water prevented detection of water that is actually *produced* by dissociative methanol chemisorption,[8,31−34] except for very small bands at ∼1610 cm^{-1} in the alumina systems (not shown).

(62) Nakamoto, K. *Infrared and Raman Spectra of Inorganic and Coordination Compounds*, 4th ed.; Wiley: New York, 1986.
(63) Bailes, M.; Stone, F. S. *Catal. Today* **1991**, *10*, 303.
(64) Suda, Y.; Morimoto, T. *Langmuir* **1987**, *3*, 786.

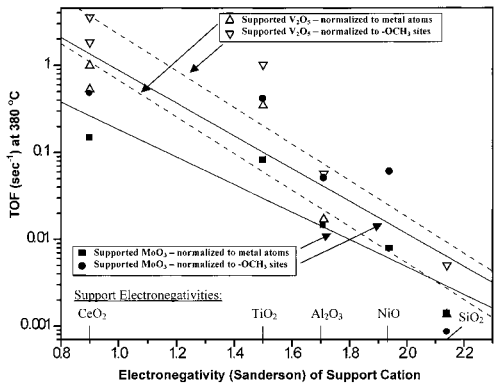

Figure 8. The support effect in supported molybdena and vanadia catalysts. Comparative calculations are made using methanol oxidation TOFs, based on total metal atoms, and TOFs based on the site densities determined by methanol chemisorption.

More detailed band assignments for the C−H stretching and bending modes in Figures 1−4 may be made according to Busca et al.[28,29] and Lavalley et al.[65] as follows. The low-frequency modes are assigned to CH_3 bending vibrations at 1450 cm^{-1} (δ_{as}) and 1430 cm^{-1} (δ_s) and to C−O stretching modes at ∼1065 cm^{-1} (ν_s). The bands at 2930 and 2830 cm^{-1} are assigned to dissociated species II and arise from Fermi resonance between the symmetric stretch (ν_s) and first overtone of the symmetric bend ($2\delta_s$) of CH_3 units in adsorbed OCH_3 species, respectively. The unusual intensity of these symmetric stretching bands is attributed to the Fermi resonance occurring between them.[29] The bands at 2950 and 2850 cm^{-1} are assigned to the same modes occurring in the undissociated species I. The less-resolved and weaker shoulder around 2970 cm^{-1} is assigned to the asymmetric stretch (ν_{as}) of the CH_3 units in these methoxylated surface species, and the broad and weak band at ∼2900 cm^{-1} is due to the overtone of the asymmetric $-CH_3$ bend ($2\delta_{as}$) in these species. Figure 2 also shows that methanol adsorption generally titrates the surface hydroxyls of the clean catalyst, as indicated by the negative bands above 3500 cm^{-1}. However, both types of methoxylated surface species are still produced in cases where the clean catalyst surface hydroxyls are either not titrated (e.g., 6% MoO_3/TiO_2 in Figure 2) or are not plentiful (e.g., $Fe_2(MoO_4)_3$[8]).

In addition to the IR spectra shown in Figures 1−3, the IR spectra in the C−H stretching region of these adsorbed methoxylated surface species are also given in Figure 4 for a series of supported-MoO_3 monolayer catalysts after methanol adsorption. The most noticeable differences in the various spectra concern the relative ratios of surface species I to species II. Generally, supported-molybdena catalysts exhibit greater or comparable band intensities of the intact, surface Lewis-bound species I relative to the dissociated surface methoxy species II. Supported-vanadia catalysts (see Figures 1 and 2) contain IR bands due almost entirely to species II, with the exception of bands from $Si-OCH_3OH$ (species I) at 2960 and 2860 cm^{-1} due to methanol adsorption on exposed silica Lewis acid sites in 10% V_2O_5/SiO_2 (Figure 2). Methoxylated surface species adsorbed on Mo or Si sites could not be distinguished in 5% MoO_3/SiO_2 because both sites apparently produce only species I in this catalyst (Figures 2 and 4). However, variation in the ratio of the two types of methoxylated surface species occurs even among the Mo-based catalysts. For example, the 2.3% MoO_3/Fe_2O_3 catalyst (Figure 4) exhibits substantial band intensities at 2930/2830 cm^{-1} due to dissociated surface methoxy species II. A summary of the vibrations of methoxylated surface species on all of the supported metal oxide catalysts tested in the present study is given in Table 1.

3.2. Quantification of Adsorbed Methoxylated Surface Species. To quantify the number of active metal oxide sites by methanol chemisorption, the IR bands associated with the methoxylated surface species (species I and II) require calibration. Beer's law dictates that the integrated area of an IR absorption band is linearly proportional to the product of analyte concentration and the beam path length through the sample.[66] The proportionality constant is often termed the integrated molar extinction coefficient, or IMEC, and in the present study, this IMEC was determined using the volumetric dosing method described by Emeis.[66]

A typical calibration and site density determination is illustrated in Figure 1, in which 5% V_2O_5/TiO_2 was employed. For this catalyst, doses of ∼5 Torr of methanol (0.86 μmol CH_3OH in the 3.19 mL dosing volume) were sequentially exposed to the sample, followed by spectrum acquisition after each dose. It is clearly seen in Figure 1 that the IR band intensities of the C−H stretching modes due to adsorbed methoxylated surface species are increasing with the number of doses. By the fifth dose, a gas-phase methanol band appears at 2981 cm^{-1} in the C−H stretching region of Figure 1, while a much stronger band appears at 1033 cm^{-1} in the C−O vibrational region (not shown). Final saturation of the sample with 10 Torr methanol, followed by evacuation of the gas phase, yields the desired saturation of the catalyst surface by adsorbed methoxylated surface species (top spectrum in Figure 1; both types of methoxylated surface species being hereafter referred to as surface methoxy species for brevity).

The IMEC values were calculated by collectively integrating the IR bands at 2830−2850 cm^{-1} in the spectra of the initial doses. These well-defined bands have relatively little overlap with other vibrational bands in the spectra and, therefore, provide the best signal for quantification. In addition, measurement of the concentrations of surface methoxy intermediates during steady-state methanol oxidation is an obvious extension of the present study and should be considered when selecting the bands to be integrated. For instance, at reaction temperatures (200−400 °C) the presence of adsorbed formate surface species (HCOO−) can produce very intense bands at 1550 cm^{-1} (O−C−O asymmetric stretch) and 1390 cm^{-1} (O−C−O symmetric stretch).[28,29] These surface formate bands, combined with less certain assignments[8] for the surface methoxy C−O vibrations and additional metal−oxygen double-bond modes in the region 980−1100 cm^{-1}, significantly complicate the quantification of adsorbed methoxy intermediates using surface methoxy bands in the low-frequency region. Higher frequency C−H stretching modes for the surface formate species also appear at 2883 and 2975 cm^{-1} but are very weak and generally are separated from the more quantifiable $2\delta_s$-(CH_3) modes of the surface methoxy species at 2850/2830 cm^{-1}.

The results of these band integrations are shown in Figure 5 for supported vanadia catalysts. It can be seen that the initial doses produce a high degree of linearity between the integrated absorbance and the known amount of methanol dosed into the cell. Such linearity and the passage of the lines through the origin indicate that methanol adsorption at 110 °C on these catalysts produces

(65) Lavalley, J. C.; Sheppard, N. *Spectrochim. Acta.* **1972**, *28A*, 2091.

(66) Emeis, C. A. *J. Catal.* **1993**, *141*, 347.

Table 1. IR Frequencies (cm^{-1}) of Adsorbed Methoxylated Surface Species on Supported Metal Oxide Catalysts after Saturation with 10 Torr of Methanol and Subsequent Evacuation (I = Species I; II = Species II)

		$\nu_s(CH_3)$			$2\delta_s(CH_3)$						
catalyst	ν_{as} (CH_3)[a]	I	II	$2\delta_{as}$[b]	I	II	δ_{as}	δ_s	δ (OH)	r (CH_3)	ν_s (CO)
20%V_2O_5/Al_2O_3	2965		2930	2888		2830	1446	1436	1385[b]	1153[b]	1073
3% V_2O_5/CeO_2	2973	2957	2931	2886	2853[b]	2826	1451	1436	1335[b]	1150[b]	1065
10% V_2O_5/SiO_2	2976		2932	2889		2831	1448	1436	c	*c*	*c*
5% V_2O_5/TiO_2	2975	2959	2935	2888	2853[b]	2830	1447	1435	1370[b]	1145[b]	1070
4% V_2O_5/ZrO_2	2975	2960	2929	2891	2854[b]	2829	1448	1437	-	1149[b]	1060
18%MoO_3/Al_2O_3	2990	2958	2926[a]	2910	2843	2831[a]	1462	1448	1385[a]	1186[b]	1065
3.5%MoO_3/CeO_2	2979	2956	2931	2888	2852[b]		1453	1439	1355[b]	1150[b]	1070
2.3%MoO_3/Fe_2O_3	2984	2955	2931	2897	2849[b]	2825	1459	1439	1360[b]	1153[b]	1048
4.3% MoO_3/NiO	2993	2960	2940[a]	2914	2854	2828	1463	1448	1364	1194[b]	1048[b] 1108
5% MoO_3/SiO_2	2996	2959	2927		2857		1473[a]	1463	c	*c*	*c*
6% MoO_3/TiO_2	2994	2961	2930	2915	2855	2836	1447	1431	1363	1178[b]	1116
4% MoO_3/ZrO_2	2984	2960	2938	2893	2853	2835	1448	1437	1370[a]	1146	1065
15%Nb_2O_5/Al_2O_3	2995	2953	2934	2896	2854[b]	2833	1457	1442	1395[a]	1153[a]	1102 1130
7% Nb_2O_5/TiO_2	2973	2948	2926	2891	2845[b]	2828	1457	1438	1370[b]		1155
5% Nb_2O_5/ZrO_2	2983	2946[b]	2927	2896		2828	1455	1439	1406[b]		1157
25% WO_3/Al_2O_3	2998	2955	2937	2907	2854	2838	1460	1448	1375[a]	1188[b]	10861158[b]
7% WO_3/TiO_2	2983	2959	2928	2985	2852	2831	1459	1445	1370		1128
17% Re_2O_7/Al_2O_3		2965			2850		1464	1452	1411	1187[b]	1081 1124
5% Re_2O_7/TiO_2	2995	2960	2930	2895	2854	2835	1455[d]	1455[d]	1360		1124
12%Cr_2O_3/Al_2O_3		2954[d]	2954[d]		2835[d]	2835[d]	*c*	*c*	*c*	*c*	*c*
5% Cr_2O_3/TiO_2	2988	2954	2926		2851	2827	1456	1430	*c*	*c*	*c*

[a] Shoulder. [b] Very weak. [c] Opaque region. [d] Broad and unresolved.

Table 2. Integrated Molar Extinction Coefficients with 95% Confidence Limits for the $2\delta_s(CH_3)$ Bands in the 2800−2850 cm^{-1} Region over Supported Metal Oxide Catalysts

Supported Metal Oxides	
catalyst	IMEC (cm/μmol)
6 wt % MoO_3/TiO_2	0.69 ± 12%
7 wt % Nb_2O_5/TiO_2	1.82 ± 4.3%
7 wt % WO_3/TiO_2	0.89 ± 2.3%
5 wt % Re_2O_7/TiO_2	0.46 ± 22%
5 wt % CrO_3/TiO_2	0.57 ± 26%
5 wt % V_2O_5/TiO_2	0.61 ± 3.0%
20 wt % V_2O_5/Al_2O_3	0.31 ± 9.6%
10 wt % V_2O_5/SiO_2	0.37 ± 19%
4 wt % V_2O_5/ZrO_2	0.55 ± 22%
3 wt % V_2O_5/CeO_2	3.01 ± 27%
18 wt % MoO_3/Al_2O_3	0.77 ± 3.9%
2.3 wt % MoO_3/Fe_2O_3	1.30 ± 5.7%
4.3 wt % MoO_3/NiO	0.99 ± 35%
5 wt % MoO_3/SiO_2	0.53 ± 1.3%
4 wt % MoO_3/ZrO_2	0.62 ± 2.8%
3.5 wt % MoO_3/CeO_2	3.37 ± 6.0%
15 wt % Nb_2O_5/Al_2O_3	0.78 ± 9.4%
5 wt % Nb_2O_5/ZrO_2	1.94 ± 5.7%
25 wt % WO_3/Al_2O_3	0.98 ± 12%
17 wt % Re_2O_7/Al_2O_3	1.38 ± 30%
12 wt % CrO_3/Al_2O_3	0.75 ± 11%

only surface methoxy species during the initial doses. Adsorption of methanol to other species or on the cell walls would have forced the lines away from the origin and most likely would have generated nonlinear calibration curves even at low surface methoxy coverage. The extinction coefficients were calculated from the slopes of these lines and are presented in Table 2 with 95% confidence limits. Figure 5 also shows that for higher doses the integrated absorbances fall below the projected line determined by the initial doses. This behavior indicates that for higher doses the methanol remains partially in the gas phase and does not completely adsorb onto the catalyst surface, which is expected for typical Langmuir equilibrium adsorption at high fractional coverages of adsorbed surface methoxy species.[50]

In fact, the equilibrium adsorption isotherm was measured at 110 °C for 3% V_2O_5/CeO_2 by exposing the sample to different saturation pressures of methanol for up to 30 min before evacuating and recording the spectrum (see Figure 6). The fractional coverage of adsorbed methoxy surface species for each data point on the isotherm was taken as the ratio of the integrated absorbance of the 2830−2850 cm^{-1} bands to the integrated absorbance at saturation. The isotherm data in Figure 6 were then best fit to Langmuir, Temkin, and Freundlich functionalities[50] to estimate the error involved in the quantitative dosing procedure employed in the present study (see the Appendix). For instance, the insert shows the lines corresponding to the IR cell mass balances for different initial doses, from which their intersection with the isotherm indicates the equilibrium surface methoxy coverage for the dose (i.e., the solution of the two equations for the two unknowns of P and θ). These calculations indicate that a dose of 5 Torr in the dosing volume, which would give a fractional surface coverage of 0.135 if all of the methanol were adsorbed (methanol vapor pressure = 0 Torr), instead equilibrates at a fractional surface coverage of 0.124 (methanol vapor pressure slightly above zero Torr). This corresponds to an error of 8%, which is quite good considering the assumptions involved in the calculations. Lower errors are obtained at low fractional surface coverages if the Temkin or Freundlich isotherms are used because these isotherms have steeper initial slopes than the Langmuir isotherm. However, the Langmuir isotherm gives a much better fit to the data at higher fractional surface coverages and, therefore, is probably the better overall isotherm functionality for the present study.

The amount of methanol chemisorbed on the catalysts after final saturation was calculated from the integrated absorbances of the saturated spectra (shown in Figure 5 at an arbitrary abscissa position) by using the IMEC values obtained from the initial doses. From these calculations it was possible to determine the catalyst active site densities (sites per m^2) and turn-over frequencies (TOFs, the activities per site). The results are summarized with 95% confidence limits in Table 3 and will be discussed in detail in the next section. In addition, it is noteworthy that the surface methoxy saturation of the 5% V_2O_5/TiO_2 catalyst used in these dosing experiments occurred at 0.34 surface methoxy molecules per V atom, which is consistent

Table 3. Site Densities (with 95% Confidence Limits) and Methanol Oxidation TOFs for Monolayer Supported Metal Oxide Catalysts (TOFs Based on Methanol Chemisorption Site Densities)[a]

catalyst	OCH_3 molecules/ metal atom	$N_m = \mu$mol metal atoms/m^2	$N_s = \mu$mol OCH_3/m^2	activity at 250 °C μmol/m^2 s	% selectivity to oxidation products	TOF at 250 °C = s^{-1}
20 wt % V_2O_5/Al_2O_3	0.30	12.2	3.64 ± 6.8%	0.42	49	0.057
3 wt % V_2O_5/CeO_2	0.29	9.16	2.68 ± 6.0%	5.10	95	1.81
10 wt % V_2O_5/SiO_2	0.27	3.43	0.93 ± 7.3%	0.005	86	0.005
5 wt % V_2O_5/TiO_2	0.34	9.99	3.44 ± 1.2%	3.46	100	1.01
4 wt % V_2O_5/ZrO_2	0.28	11.3	3.16 ± 9.0%	11.3	99	3.53
18 wt % MoO_3/Al_2O_3	0.28	7.73	2.18 ± 2.1%	0.23	49	0.052
3.5 wt % MoO_3/CeO_2	0.17	8.10	1.41 ± 1.6%	0.21	87	0.13
2.3 wt % MoO_3/Fe_2O_3	0.78	7.62	5.92 ± 4.6%	0.30	100	0.051
4.3 wt % MoO_3/NiO	0.13	7.39	0.96 ± 14%	0.07	82	0.060
5 wt % MoO_3/SiO_2	1.59	2.17	3.46 ± 0.8%	0.006	49	0.0009
6 wt % MoO_3/TiO_2	0.20	6.82	1.35 ± 4.3%	0.68	82	0.41
4 wt % MoO_3/ZrO_2	0.31	5.24	1.61 ± 1.9%	0.77	100	0.48
15 wt % Nb_2O_5/Al_2O_3	0.38	6.27	2.37 ± 5.7%	1.74	0.00	0.00
7 wt % Nb_2O_5/TiO_2	0.42	9.58	4.02 ± 1.7%	0.076	2.50	0.0005
5 wt % Nb_2O_5/ZrO_2	0.33	9.65	3.18 ± 1.4%	0.087	0.00	0.00
25 wt % WO_3/Al_2O_3	0.29	5.98	1.73 ± 4.8%	acidic	0.00	0.00
7 wt % WO_3/TiO_2	0.45	5.48	2.49 ± 0.6%	acidic	0.00	0.00
17 wt % Re_2O_7/Al_2O_3	0.50	3.91	1.96 ± 8.2%	n/a[b]	n/a	n/a
5 wt % Re_2O_7/TiO_2	0.40	3.97	1.58 ± 9.8%	1.08	93	0.64
12 wt % CrO_3/Al_2O_3	0.59	6.68	3.91 ± 2.8%	n/a	n/a	n/a
5 wt % CrO_3/TiO_2	0.54	9.09	4.95 ± 6.2%	0.65	89	0.12

[a] Note that TOF = [(activity)(selectivity)]/N_s. [b] n/a = not available.

Table 4. Relative Fractionation of Species I vs Species II in Titania-Supported Metal Oxide Catalysts[a]

	deconvolution and Curve Fitting:			simple integration (from Table 3):
catalyst	species II/ metal atom	species I/ metal atom	OCH_3 molecules/ metal atom	OCH_3 molecules/metal atom
5 wt % V_2O_5/TiO_2	0.34 (94%)	0.02 (6%)	0.36	0.34
6 wt % MoO_3/TiO_2	0.14 (67%)	0.07 (33%)	0.21	0.20
7 wt % Nb_2O_5/TiO_2	0.36 (95%)	0.02 (5%)	0.38	0.42
7 wt % WO_3/TiO_2	0.31 (74%)	0.11 (26%)	0.42	0.45
5 wt % Re_2O_7/TiO_2	0.30 (77%)	0.09 (23%)	0.39	0.40
5 wt % CrO_3/TiO_2	0.30 (58%)	0.22 (42%)	0.52	0.54

[a] Beer's law: $[IA]_A = \epsilon_A n_A(1/\pi r^2)$: $[IA]_B = \epsilon_B n_B(1/\pi r^2)$. $[IA]_i$ are integrated absorbances. ϵ_i are IMECs; n_i are moles. Mass balance: $n_A + n_B = n_T$. Substituting $\{(1/\epsilon_A)\pi r^2[IA]_A\} + \{(1/\epsilon_B)\pi r^2[IA]_B\} = n_T$, where n_T, $[IA]_A$, and $[IA]_B$ are measured in the dosing experiment. Data in table are the result of calculations employing the above equations and assuming $\epsilon_A = \epsilon_B$ (see text).

with recent thermogravimetric (TGA) results under similar nonoxidizing, static conditions.[67] Furthermore, the same surface methoxy saturation value for 5% V_2O_5/TiO_2 was obtained when the TGA experiment was repeated on compressed IR wafers (instead of the usual 75 μm powders)—indicating that the process of compressing the catalyst powders into thin IR wafers does not affect the microporosity or number of accessible sites.

3.3. Fourier Self-Deconvolution of Titania-Supported Catalysts. An important refinement in these calculations is presented in Figure 7 and Table 4, in which the site densities of methoxylated surface species I and species II were determined separately for titania-supported catalysts for use in comparing the relative reactivities of these species (see Discussion section). These calculations were especially difficult for the supported vanadia and niobia systems because the band at 2850 cm^{-1}, due to species I, appeared only as an unresolved shoulder in these catalysts. Curve fitting was attempted using several different line shapes, but reliable results were only obtained when the raw spectra were first enhanced by using a Fourier self-deconvolution (FSD) routine. The FSD technique has been well-described by Kauppinen et al.[68] and involves deconvoluting the intrinsic line shape, taken as Lorentzian, from the raw spectra. Mathematically, the inverse Fourier transform of the Lorentzian profile is divided out of the inverse Fourier transform of the raw data (the interferogram), and subsequent Fourier transformation of the resulting modified interferogram yields an enhanced spectrum with narrower bandwidths. If "perfect" deconvolution could be achieved the enhanced spectral bands would have the instrument line shape, which in this case is the Bessel apodization function. However, line shapes are more often composed of both Lorentzian and Gaussian components, so curve fitting of the deconvoluted spectra is still required and works best using Voigt profiles (convolution of Gaussian and Lorentzian line shapes). All FSD and curve-fitting calculations were performed using the Bio-Rad Win-IR with GRAMS/32 software package (Galactic Industries Corp.).

The results of performing FSD and Voigt profile curve fitting are presented in Figure 7 for 5% V_2O_5/TiO_2. The separate integrations of the 2850 and 2830 cm^{-1} bands allow for calculation of the individual site densities for methoxylated surface species I and species II. While it is also possible to estimate individual extinction coefficients by least-squares methods (see Table 4 notes), the error involved proved prohibitive. Therefore, both bands were assumed to have the same IMEC due to their similar frequencies and molecular origins. These IMEC values were calculated (see Table 4 notes) to be, on average, 18% higher than the IMEC values reported in Table 2. Such an inflation in the IMECs is typical for spectra that have

(67) Briand, L. E.; Wachs, I. E. 1998. Unpublished results.
(68) Kauppinen, J. K.; Moffatt, D. J.; Mantsch, H. H.; Cameron, D. G. *Appl. Spectrosc.* **1981**, *35*, 271.

undergone FSD,[69] and illustrates that IMEC values obtained from self-deconvoluted spectra should only be considered as internal calibrations and not as representative of the true molecular absorptivities. The individualized surface methoxy site density results for the other titania-supported catalysts, which were chosen because they possess relatively well-defined surface methoxy bands and also exhibit changes in the ratio of species I to species II for different deposited metal oxides, are summarized in Table 4. No attempt has been made to calculate TOFs on the bases of the site densities of the individual species because both species are likely involved in methanol oxidation (see Discussion section). Consequently, the TOFs in Table 3 were calculated using the *total* surface methoxy site densities obtained by integrating all bands in the *region* 2800−2850 cm^{-1}.

4. Discussion

The results presented above have both qualitative and quantitative applications toward the development of fundamental structure−reactivity relationships for methanol oxidation over metal oxides. Qualitatively, methanol chemisorption proceeds by two different pathways. The first pathway adsorbs methanol associatively to produce an intact Lewis-bound adsorbed surface methanol species (species I) that remains stable to relatively high temperatures under vacuum (100−200 °C, at least). The second pathway dissociatively adsorbs methanol to form surface methoxy species (−OCH_3, species II) and surface hydroxyls. In both cases, the methoxyl-group oxygen is coordinated to a surface Lewis acid cation, while in the dissociated case the methanol alcoholic proton must coordinate to a basic surface oxygen anion or to a surface hydroxyl (producing either surface hydroxyls or water, respectively). Generally, all hydroxyls present on the clean catalysts (>3500 cm^{-1}) are titrated upon saturation of the surface with adsorbed methoxylated surface species, and new bands at 3100−3500 cm^{-1} are created by the presence of an OH group within intact Lewis-bound species I. Importantly, Lewis-bound water (∼1610 cm^{-1}) is rarely observed even at saturation and any residual water on the metal oxide surfaces present prior to methanol exposure is displaced by the adsorbed methoxylated surface species. Surface hydroxyls are generally present at much lower levels in cases where primarily dissociated species (species II) are formed (see Figures 2 and 3), indicating their condensation and evolution from the surface as water.

Similar conclusions about these dual adsorption pathways and the evolution of water from the metal oxide surfaces have been drawn by Suda et al.,[42] Farneth et al.,[31−33] Busca et al.,[29] and others.[35,36,39] These studies and the present results clearly indicate that quantitative chemisorption measurements must either measure the methoxylated surface species directly by IR spectroscopy (CeO_2,[43] ZnO,MgO,[37] MoO_3,[44] SiO_2,[38] and ZrO_2[51]), or measure the water desorbed upon adsorption if gravimetric methods are used.[31−33,42] However, the absence of Lewis-bound water after methanol chemisorption on virtually all catalysts tested in the present investigation suggests that higher temperature methanol chemisorption (110 °C) forces the water equilibrium toward the vapor phase and allows for the assumption of complete water loss (relevant to gravimetric methods).

Interestingly, Table 2 indicates a significant variation in the IMEC values for adsorbed methoxylated surface species on the different supported metal oxide catalysts. In particular, the supported-Nb_2O_5 catalysts and the CeO_2-supported catalysts have two to three times the IMEC values, respectively, as those of the other samples. These variations most likely arise from the effects of radiation scattering, support composition, support particle size, loading level of dispersed oxide, and other factors. Nevertheless, Table 3 shows that the CeO_2-supported catalysts have extremely high methanol oxidation activity toward oxidation products, whereas supported-Nb_2O_5 catalysts are active only toward acidic products. Therefore, there does not appear to be an obvious connection between the IMEC values and methanol oxidation TOFs. The IMECs reported in Table 2 are given primarily as illustration of the methodology used for signal calibration, although they could also be used as starting points for future work regarding the molecular origins of the IMEC variations in adsorbed methoxylated surface species.

The quantitative measurement of the methoxylated surface site densities (see Table 3) further shows that supported metal oxide catalysts are sterically limited to about 0.3 methoxylated surface molecules per active metal atom. Even for supported niobia, chromia, and rhenia catalysts, in which the total site density per metal atom is slightly higher at about 0.5 methoxylated surface molecules per metal atom, the individual site densities for methoxylated surface species I and species II never exceed 0.36 methoxylated intermediates per metal atom (see Table 4). The MoO_3/SiO_2 and V_2O_5/SiO_2 systems, which cannot achieve full monolayer coverage due to the low reactivity of SiO_2 with the dispersed metal oxides, are also quite interesting. In particular, the V−OCH_3 IR bands could be easily distinguished from the Si−OCH_3 bands and similarly indicate 0.27 methoxylated surface intermediates adsorbed per vanadium cation (methoxylated surface intermediates per Si site cannot be determined because the number of exposed Si cations is unknown). However, in 5% MoO_3/SiO_2 the Mo−OCH_3 and Si−OCH_3 IR bands are coincident and yield an artificially inflated value of 1.59 methoxylated surface intermediates per Mo cation because the Si−OCH_3 species are necessarily included in the band integrations. An analogous inflation of Re−OCH_3 species may also be occurring in supported-rhenia catalysts due to the inability of these catalysts to achieve full monolayer coverage as a result of dimerization and volatilization of the dispersed rhenia species above about one-half monolayer surface coverage.[6]

Fortunately, the other monolayer catalysts presently studied do *not* exhibit exposed support sites and, as desired, produce methoxylated surface intermediates coordinated only to the dispersed metal oxide metal atoms. This is sometimes supported by distinctly different IR band positions for the methoxylated surface species on the monolayer catalysts compared to those on the pure oxide supports (e.g., MoO_3/Fe_2O_3 vs Fe_2O_3; see part 2[8]). However, additional evidence is found in previous methanol oxidation transient experiments,[16] in which methanol is suddenly removed from a continuous gas flow at reaction conditions followed by observation with in-situ IR for the presence or absence of unreactive spectator methoxylated surface species. The oxide supports are known to require much higher temperatures to catalyze methanol oxidation than the monolayer catalysts,[8] so methoxylated surface species adsorbed on exposed support sites would be expected to act as unreactive spectators at the much lower temperatures used in the transient experiments with monolayer catalysts. These studies indicated that such unreactive spectator species are generally not present at

(69) Czarnecki, M. A.; Ozaki, Y. *Spectrochim. Acta Part A* **1996**, *52*, 1593.

monolayer coverages (silica-supported and supported-rhenia catalysts being the exceptions, as described above).

The TOF for methanol oxidation must now be redefined by taking the density of methoxylated surface species at saturation as the number of active surface sites, since less than half of the total deposited metal oxide sites can simultaneously participate during steady-state methanol oxidation in supported metal oxide catalysts. In previous studies, the total number of deposited metal atoms present in the two-dimensional metal oxide overlayer was taken as the number of active sites,[21] which allowed for extremely useful *relative* comparisons of intrinsic activities between catalysts but poses difficulties for kinetic modeling. Specifically, recent in-situ IR studies of methanol oxidation over supported metal oxide catalysts have revealed that the fractional surface coverage of methoxylated surface intermediates relative to saturation coverage is between 0.3 and 0.68 under steady-state reaction conditions when methanol chemisorption site densities are used to define the saturation coverage.[70] Conversely, fractional coverage is generally less than 0.2 when total dispersed metal oxide metal atoms are used to define saturation coverage. Many previously developed kinetic models often assume this low surface coverage limit when taking the surface area or total number of deposited metal atoms as the total site density.[30] Therefore, the use of methanol chemisorption site densities is more appropriate for kinetic modeling, where it can no longer be assumed that methanol oxidation over oxides proceeds exclusively within the low surface coverage regime.

The effect of redefining TOF using methanol chemisorption surface site densities is illustrated graphically in Figure 8, where it can be seen that the new TOFs for both supported molybdena and vanadia catalysts are higher than the metal oxide-based TOFs. This is expected because, for a given activity per m^2, the methanol chemisorption site densities N_s are lower than the densities of metal atoms in the deposited surface metal oxides N_m (see Table 3). Nevertheless, the support effect observed previously[10,11,21] using the metal oxide-based TOFs remains virtually unchanged as a general trend by the use of the new methanol chemisorption surface site densities. This is also shown in Figure 8, where apparent linear regression lines are fitted to the TOFs of supported vanadia and molybdena catalysts using both definitions of site density. While the linear fits are only crude representations of the somewhat scattered data in this semilog plot, they do serve to point out that redefining the TOF with methanol chemisorption surface site densities simply scales the TOFs upward by a factor of ~3. Very little difference is observed in the slopes of the lines, except that supported vanadia exhibits a slightly greater support effect due to its higher TOFs in both definitions. This means that the total number of metal atoms in the deposited surface metal oxides are still proportional to the actual number of active surface sites as measured by methanol chemisorption. Such proportionality is, in turn, due to the steric limitation of 0.3 methoxylated surface species per metal atom that appears to be relatively constant for the majority of the supported metal oxide catalysts.

Current explanations of this support effect in supported metal oxide catalysts and the correlation with support cation electronegativity generally focus on the bridging M−O−Support bond (M = Mo, V, etc.) as the critical active site.[19−21] The molecular structures of the active surface metal oxide species on calcined, dehydrated, and fully oxidized supported metal oxide catalysts consist of an MO_4 or MO_6 unit possessing a single M=O (mono-oxo) terminal bond, bridging M−O−Support bonds, and polymerized M−O−M bonds at higher loading in some systems.[5,6] Numerous experimental[9,19−22] and theoretical[71,72] studies indicate that the bridging M−O−Support bond is the active site for dehydrogenation, and an appropriate fundamental property of this local bond—the electronegativity of the support cation—is generally taken to be representative of the catalytic behavior of this bond. Preferably, the Sanderson electronegativy is used because of its better handling of the "inert pair effect" associated with nonbonding d-electrons in transition metal oxides,[73] and values have been tabulated for many main group and transition metals in various oxidation states.[73] The electronegativity of the support cation has already been successfully correlated to TOF in supported vanadia catalysts using TOFs calculated with total dispersed metal oxide metal atoms for active surface site densities,[21] so the replication in Figure 8 of the same general trend in support effect using *methanol chemisorption* site densities aids in validating the methanol chemisorption technique. A critical conclusion stemming from this result is that the methanol chemisorption methodology presented in the present study may now be extended with confidence to search for similar ligand effects in bulk metal oxides, where counting active sites has traditionally been very difficult (subject of part 2[8]).

Finally, it is interesting to observe from Table 4 that titania-supported niobia and vanadia possess almost exclusively the dissociated form of adsorbed methoxy species (species II). Substantially greater amounts of Lewis-bound species I are present in the other systems. Ouyang et al.[51] found that surface methoxy species adsorbed on terminal and bridged zirconia sites may be interconverted, and Table 3 shows that titania-supported niobia and vanadia exhibit greatly different reactivities despite possessing very similar surface methoxy species. Therefore, differences in the redox behavior of the bridging M−O−Support bond in the active metal oxides seem to be more important for determining overall redox activity than the ratio of methoxylated surface species I to species II. Conversely, the different ratios of methoxylated surface species may be related to formaldehyde selectivity, which is especially relevant to molybdena and vanadia catalysts. Low selectivity is obtained at high conversions only in vanadia-based catalysts due to the readsorption of formaldehyde product on vanadia sites and their further oxidation to carbon oxides.[3,4] Therefore, it is possible that the presence of intact, strongly Lewis-coordinated methanol species (species I) prevents or blocks the readsorption of formaldehyde product in molybdena catalysts at high conversions.

5. Conclusions

The present study has demonstrated that high temperature (110 °C) methanol chemisorption combined with infrared spectroscopy is a reliable and powerful technique for determining the surface density of active metal oxide sites in methanol oxidation catalysts. Quantitative doses of methanol at low surface coverages allow for the

(70) (a) Burcham, L. J. *Ph.D. Dissertation*; Lehigh University: Bethlehem, PA, 2000; Chapter 5. (b) Burcham, L. J.; Badlani, M.; Wachs, I. E. *J. Catal.* **2000**. Submitted for publication.

(71) Weber, R. S. *J. Phys. Chem.* **1994**, *98*, 2999.

(72) Tran, K.; Hanning-Lee, M. A.; Biswas, A.; Stiegman, A. E.; Scott, G. W. *J. Am. Chem. Soc.* **1995**, *117*, 2618.

(73) (a) Sanderson, R. T. *J. Chem. Educ.* **1988**, *65*, 112. (b) Sanderson, R. T. *Inorg. Chem.* **1986**, *25*, 3518.

measurement of integrated molar extinction coefficients of adsorbed methoxylated surface species, which are then used to calculate the saturation site densities from the corresponding integrated IR band absorbances (2830−2850 cm^{-1}) in the saturated spectra. Furthermore, the presence of two distinct adsorbed phases is indicated by the IR spectra. The first phase is an intact, Lewis-bound surface methanol species (species I) and the second phase is a dissociated surface methoxy species (−OCH_3, species II). Adsorption of methanol on these surfaces is generally accompanied by the gaseous evolution of surface water, although the exact stoichiometry of the water production is not required when quantifying adsorbed methoxylated surface species *directly* with IR spectroscopy. The amount of physisorbed methanol and physisorbed water has also been minimized by performing the methanol chemisorption at elevated temperature and under vacuum.

Measurements of surface site densities in supported metal oxide catalysts indicated a steric limitation of about 0.3 surface methoxylated intermediates per active metal atom across all supported metal oxides and led to recalculation of methanol oxidation TOFs using the density of methoxylated surface species at saturation as the number of active sites. The effect of redefining TOF using methanol chemisorption surface site densities increases the TOFs by a factor of ∼3 relative to the previous metal oxide-based values. Nevertheless, the support effect observed previously (TOFs for MoO_3 and V_2O_5 supported on oxides of Zr ∼ Ce > Ti > Al ≫ Si) remains virtually unchanged as a general trend and correlates with the support cation electronegativity (Figure 8). Bridging M−O−Support bonds are proposed as the active centers most likely to account for this support effect. Variations in the ratios of methoxylated surface species I to species II further suggest that the presence of intact, strongly Lewis-coordinated methanol species (species I) may prevent or block the readsorption of formaldehyde product in molybdena catalysts at high conversions to account for the favorable selectivity behavior of these systems.

Application of this methanol chemisorption/infrared spectroscopy technique can now allow methanol oxidation TOFs to be calculated on many bulk metal oxide systems previously limited to normalization only by surface area (i.e., specific activity). Such an extension is the subject of part 2[8] of this series, in which commercially relevant, mixed-metal bulk molybdates are studied by methanol chemisorption and methanol oxidation.[8] Moreover, and beyond their already critical role in calculating TOFs, the surface site density measurements also have an impact on the kinetic modeling of the methanol oxidation reaction. This is because the steady-state concentrations of adsorbed methoxylated surface intermediates during methanol oxidation have recently been shown[70] to exceed the linear low coverage limit of the Langmuir isotherm frequently used by other authors in the kinetic modeling of methanol oxidation.[30] Additional structure−reactivity relationships and fundamental insights will hopefully develop from the further application of this methanol chemisorption/infrared technique.

Acknowledgment. The authors gratefully acknowledge the United States Department of Energy, Basic Energy Sciences (Grant DEFG02-93ER14350), for financial support of this work.

Appendix

The adsorption isotherms and mass-balances in Figure 6 are constructed from the following equations:

Isotherms [50]: (1) (Langmuir) $$\theta = \frac{KP}{1 + KP} \quad (1)$$

(2) (Temkin) $$\theta = \frac{1}{f}\ln(KP) \quad (2)$$

(3) (Freundlich) $$\theta = KP^{1/n} \text{ for } n > 1 \quad (3)$$

In these equations θ is fractional surface coverage, P is the equilibrium vapor pressure, and K, f, and n are fitted constants.

Mass-balance for methanol in the IR cell:

moles gas = moles gas (initial) − moles (adsorbed) (4)

$$n_{gas} = n_{gas,o} - \left(n_{ads,sat}\frac{n_{ads}}{n_{ads,sat}}\right) = n_{gas,o} - (n_{ads,sat}\theta) \quad (5)$$

using the ideal gas-law: $$\theta = \left(\frac{V}{RT}\right)(P_o - P)\frac{1}{n_{ads,sat}} \quad (6)$$

In this equation θ and P are defined as before, R is the gas constant, T is the absolute temperature, and $n_{ads,sat}$ is the molar amount of methanol adsorbed on the oxide surface at saturation. The symbol V is the combined volume of the IR cell and dosing volume, and this quantity was determined by measuring the pressure change exhibited upon venting a known amount of ideal gas (air) originally in the calibrated dosing volume into the evacuated IR cell. Finally, P_o is the initial pressure in this total volume V for a given dose, which is calculated from the ideal gas law using the known moles of methanol as determined from the original pressure in the dosing volume before exposure to the IR cell.

LA010009U